HHS Public Access

Author manuscript

Proc SPIE Int Soc Opt Eng. Author manuscript; available in PMC 2017 February 27.

Published in final edited form as:

Proc SPIE Int Soc Opt Eng. 2016 February 27; 9784: . doi:10.1117/12.2212805.

Unsupervised fetal cortical surface parcellation

Sonia Dahdouh[a] and **Catherine Limperopoulos**[a]

[a]Children's national medical center, 111 Michigan Ave NW, Washington DC 20010, USA

Abstract

At the core of many neuro-imaging studies, atlas-based brain parcellations are used for example to study normal brain evolution across the lifespan. These atlases rely on the assumption that the same anatomical features are present on all subjects to be studied and that these features are stable enough to allow meaningful comparisons between different brain surfaces and structures These methods, however, often fail when applied to fetal MRI data, due to the lack of consistent anatomical features present across gestation. This paper presents a novel surface-based fetal cortical parcellation framework which attempts to circumvent the lack of consistent anatomical features by proposing a brain parcellation scheme that is based solely on learned geometrical features. A mesh signature incorporating both extrinsic and intrinsic geometrical features is proposed and used in a clustering scheme to define a parcellation of the fetal brain. This parcellation is then learned using a Random Forest (RF) based learning approach and then further refined in an alpha-expansion graph-cut scheme. Based on the votes obtained by the RF inference procedure, a probability map is computed and used as a data term in the graph-cut procedure. The smoothness term is defined by learning a transition matrix based on the dihedral angles of the faces. Qualitative and quantitative results on a cohort of both healthy and high-risk fetuses are presented. Both visual and quantitative assessments show good results demonstrating a reliable method for fetal brain data and the possibility of obtaining a parcellation of the fetal cortical surfaces using only geometrical features.

1. INTRODUCTION

Neuro-imaging studies often use the assumption that distinct brain regions can be identified and analyzed in a consistent way on all brains that are analyzed. Surface-based analysis of the cortex is often used to study normal cerebral cortical development and evolution across the lifespan and the impact of neurodegenerative diseases on cortical integrity. This type of approach, based on a time-consuming surface registration through diffeomorphisms and guided by anatomical features such as sulcal depth and cortical curvature,[1, 2] often fail when dealing with fetal MRI data. Indeed, fetal brain development is very prolific throughout pregnancy[3] and anatomical features do not remain consistent across gestation. As illustrated in Figure 1, brain features evolve with increasing gestational age and classical landmarks such as sulci are not reliable throughout gestation as they do not exist early in gestation, but appear gradually. Moreover, the age of appearance of these landmarks tend to vary from one patient to another.

Corresponding authors: CLimpero@childrensnational.org.

The ability to define an anatomically coherent parcellation that is consistent and stable throughout all ages remains an ongoing challenge While the parcellation of the cortical surface into brain lobes can be justified throughout gestation, the use of a higher number of parcels, as is done for adult brain atlases, raises the question of what the anatomical meaning of these parcels is, as the anatomical regions are not yet differentiated in the developing fetal brain.

To address the issue of lack of temporally coherent landmarks, manually delineated sulcal landmarks have been used by Auzias *et al.*[4] as constraints in a model-driven parameterization scheme. To counter-balance the lack of many of the sulci landmarks at the earlier gestational ages,[5] additional geometric constraints such as the barycenter of the most anterior and most posterior points of the cortex are used. In the work by Pepe *et al.*,[6] spectral clustering based on the computation of the *Laplace-Beltrami* eigenfunctions computed on the cortical surface is used to define a parcellation of the brains to be segmented, and the resulting maps are then mapped into a common spherical space to perform parcels matching. While this method presents interesting results, the reproducibility appears to depend on the number of regions used in the spectral clustering procedure, and the authors suggest using a number equal to 6 or 7 parcels.

The use of such geometry-aware features has become increasingly popular for adult brain matching[7] (combined with anatomical features) or non-rigid shape matching.[8] A major drawback of the descriptors based on the eigenfunctions and eigenvalues of the *Laplace-Beltrami* operator is their ambiguity to sign flips for each eigenfunction which requires a reordering of the spectra.[9] In order to circumvent this issue, the *Heat Kernel Signature* (HKS) has been proposed.[10] Based on the heat kernel, a solution of the heat equation, the HKS is a collection of low-pass filters, thus dominated by the lower frequencies which limits its ability to precisely localize features within one shape.[9] To enhance spatial localization, a descriptor based on the *Schrödinger* equation governing the temporal evolution of quantum mechanical particles, the *Wave Kernel Signature* (WKS), was proposed by Aubry *et al.*[11] As a collection of delta filters in the Fourier domain, the WKS descriptor allows a better spatial resolution than HKS. Both HKS and WKS achieve state-of-the-art performance in shape analysis.[9]

In order to overcome the lack of consistently present anatomical brain features across all gestational ages, and in order to provide an age-independent consistent parcellation of the fetal brain, we propose to take advantage of the good discrimination properties of the WKS. The aim here is to propose a method that allows a comparison of the different regions of the cortical surface without any assumptions on anatomical features.

A new mesh signature, based on both the WKS and the Euclidean coordinates of the nodes of the mesh, is used in a k-means clustering scheme to define a consistent segmentation on a set of fetal cortical surfaces. These parcellations are then learned using Random Forests.[12] New cortical surfaces can then be parcellated and are further refined using an alpha-expansion graph-cuts framework.[13] Qualitative and quantitative assessment of the reproducibility and stability of our parcellation scheme across individuals for different cluster numbers and at different ages is then performed.

2. METHOD

2.1 Mesh signature

In order to compute a consistent signature for all the surfaces to be studied, one surface is chosen as reference and the others are roughly registered to it using a Principal Component Analysis on the normal field of the mesh. All meshes are then re-scaled to the unit box.

Let $G = \{V,A\}$, the graph built from the set of vertices V and edges A of a closed surface model $S \subset R^3$. The rationale behind the WKS computation is to characterize each node $x \in V$ by the probability $WKS_e(x)$ to measure a quantum particle with an initial energy distribution $f_e(v)$ on this point. e represents the energy level, which is directly related to the eigenvalues of the *Laplace-Beltrami* operator, giving thus an intrinsic interpretation of the shape. f belongs to a family of log-normal energy distributions.

For each point on the surface, we can thus associate a wave kernel signature of the form:[9]

$$\mathrm{WKS}_N(x) = (\mathrm{WKS}_{e_1}(x), \ldots, \mathrm{WKS}_{e_N}(x))^T \quad (1)$$

where N is the number of evaluation energies of the WKS and $e_1, \ldots, e_N$ are logarithmically sampled.

While the WKS vector demonstrates good localization performances, the sole use of it in a clustering scheme would result in spatially disconnected clusters, given that different points of the mesh can present similar WKS descriptors. Although useful for finding similar parts in the segmentation of articulated shapes, this feature becomes problematic when dealing with brain parcellation where spatial connectivity has to be enforced.

We subsequently decided to combine the *intrinsic* information provided by the WKS with the *extrinsic* one provided by the spatial coordinates of the nodes of the mesh in a unique signature of the meshes to be studied. The mesh signature can then be written as:

$$\mathrm{sig} = \{x, k \times \mathrm{WKS}_N(x)\} \quad (2)$$

with k a parameter to balance both spatial and WKS features. Indeed, without it, the greater number of evaluation energies we use, the less the impact of the spatial coordinates in the final signature, which would lead us to decrease or discard the spatial localization ability.

To obtain a signature taking both types of information into account, we decided to set k to $\frac{1}{N}$.

2.2 Cortical surfaces parcellation learning and inference

2.2.1 Cortical surfaces parcellation learning—Since the aim here is to propose a consistent parcellation of the fetal brain throughout gestation and a brain matching method

to propagate this parcellation, we decided to build the parcellation simultaneously on all the brains of a learning set instead of building it independently on each brain.

As described previously, a brain signature is defined as a collection of feature vectors computed on each node of the cortical mesh. A training set signature *tr* is then defined as an unordered collection of *m* brain signatures *sig* in R^{N+3}.

$$\mathrm{tr}=\{\mathrm{sig}_1,\ldots.,\mathrm{sig}_m\} \quad (3)$$

Noteworthy, there is no assumption made on the number of nodes of the training set meshes, each sig_i being of a different size $|V| \times (N + 3)$.

This training set is then clustered using the K-means++ algorithm.[14] Figure 2 illustrates the result of this clustering on brains at different gestational ages.

Once this clustering is performed, the parcellation needs to be propagated to new cortical surfaces. Many learning techniques could be used to perform this task. Among them, RF[12] have received increasing attention due to the appealing trade off between efficiency, computational time, and ease of use. For example, RF has been used by Lombaert *et al.*[15] to classify adult cortical surface data represented by their spectral coordinates combined with sulcal depth information. Such anatomical information, and thus the method cannot be reliably applied to fetal data as sulcal features are not stable across ages. Meng *et al.*[16] parcellated adult cortical surfaces by first registering surfaces using spherical demons and then learning Haar-like features using an incremental RF learning framework. The resulting parcels are then further refined using a curvature guided graph-cut procedure, using the assumption that curvature is a guiding force in manual segmentation for cortical data. This method thus relies strongly on the quality of the first registration, which is less reliable on fetal data as typical features such as sulcal depth cannot be used to guide it. Moreover, the assumption that changes in curvature allow a consistent separation of parcels on cortical surfaces is less straightforward. Indeed, due to brain growth, a same region at different ages can be completely smooth or fully gyrified, thus presenting really different curvature features.

Consequently, RF are extended here to use the mesh signatures defined earlier to both learn and infer the parcellation of the cortical surface. The idea is that an ensemble of decision trees makes probabilistic decisions on an input data set. In the training phase, multiple decision trees are grown by finding for each node the binary test that best splits the training data set, represented here by its vector of signatures *tr*. In the testing phase, nodes (represented by their signature *sig*) are classified using the maximum of the votes. As we can see in Figure 3 (a) and (b), this clustering produces a reasonable parcellation of the brain.

However, some disconnected regions still appear and need to be removed.

2.2.2 Cortical surfaces parcellation refinement—The aim of this final step is twofold; first to remove the non-connected components so that each parcel represents a unique connected cluster; and second, to smooth boundaries between the different parcels

making them adhere to local mesh features. Inspired by previous work by Shapira *et al.*[17] to obtain a final segmentation of non-rigid shapes based on the results of an Expectation-Maximization segmentation process on the faces of the mesh, we decided to use an alpha-expansion graph-cut method on the graph of labeled nodes to determine the final cortical parcellation. As mentioned previously, refinement based on an alpha-expansion graph-cut method on the graph of labeled nodes of cortical surfaces has also been performed.[16]

While the maximal voting provided by the Random Forest has been used to determine the initial segmentation, in the refinement process, a *probability map* P is computed from the voting information provided by all the trees for every point.

We can thus define the energy function to be minimized by the graph-cut optimization as:

$$E=\sum_{x\in V} g_1(x,l)+\lambda \sum_{\{l,d\}\in L} g_2(l,d) \quad (4)$$

$$g_1(x,l)=-\log(P(x|l)+\varepsilon)$$

$$g_2(l,d)=\begin{cases} \dfrac{\sum_{a_{l,d}\in A} -\log(\frac{\Theta(a_{l,d})}{\pi})}{|A_{l,d}|}, & l\neq d \\ 0, & l=d \end{cases}$$

with l, the label assigned to node x, L, the set of all possible labels, λ, a parameter defining the degree of smoothness, $\Theta(a)$, the dihedral angle of edge a, $a_{l,d}$, the edge where the first point belongs to cluster l and the second one to cluster d and $A_{l,d}$ the set of edges where one of the points belongs to cluster l and the second one to cluster d. In contrast to Shapira *et al.*,[17] the smoothness term is not computed for each node but a global label transition information determined on the whole training set is used; g_2 is only computed once on the whole training set. Using this refinement, spatial separation of clusters is enhanced as shown in Figure 3 (b) and (d).

2.2.3 Quantitative evaluation—The reproducibility, stability and accuracy of the proposed automated parcellation and learning framework are assessed quantitatively through the use of the measurement described below.

Parcellation reproducibility: In order to assess parcellation reproducibility, we define the reproducibility value $D_R(K)$ of a cortical parcellation with K clusters as the mean over all subjects of pair-to-pair Dice measurements as defined next.

$$R(K)=\frac{1}{M}\sum_{p,q,p\neq q} \mathrm{Dice}(p,q) \quad (5)$$

with p, q label maps with K parcels, M the number of subjects, and Dice, the usual Dice value between two different sets.

3. RESULTS

3.1 Data and pre-processing

Our database is composed of 218 fetal MRI scans with gestational ages ranging from 20 to 37 weeks: 110 MRI studies from healthy control fetuses, and 108 fetuses diagnosed with complex congenital heart disease, which has been previously shown to alter the cortical gyrification process.[18] All the scans have been semi-automatically segmented as described by Clouchoux *et al.*[3] Two different processes have been involved for the surface reconstruction. First, brain surfaces were reconstructed using *BrainSuite*[19] which provides us a set S_1 of cortical surfaces with different number of nodes and topologies. In order to be able to compare parcellation results, a subset $S_2 \subset S_1$ of 38 brains (26 controls and 12 cases) were reconstructed and registered using the method proposed and validated by Clouchoux *et al.*[3] While not perfect, the registration proposes a common ground to compare parcellation results on the different surfaces. This subset will thus constitute the testing set, as the registration process gives us a one-to-one correspondence between all the nodes of the different brains, allowing us the computation of performance metrics on the parcellation.

3.2 Qualitative validation

Figure 4 shows parcellation results at different ages and for different cluster numbers. Visual parcellations are consistent across gestational ages and cluster numbers. As a comparison, while the brain parcellations proposed by Pepe *et al*[6] seem consistent for a low number of clusters ($K \leq 7$) the error rate increased quickly for higher number of parcels. Noteworthy, the parcellation obtained with a number of clusters equal to 5 could be anatomically related to a parcellation of the brain into frontal, temporal and occipital lobes, with the frontal lobe sub-segmented into its most frontal and posterior parts.

Since we are dealing with fetal brains where sulci and gyri have not been formed yet, the use of these landmarks to define an anatomically correct parcellation into more than the main lobes remains an open question. Indeed, due to the absence of relevant anatomical landmarks throughout gestation, a highly parcellated fetal brain at one age cannot be consistently mapped to a fetal brain at another age with the assumption that corresponding regions will have the same function. However, in order to study growth trajectories or pathologic conditions, we might need a finer parcellation of the surfaces with a stable label correspondance accross all considered brains.

Thus, in the next section, we will investigate quantitatively the performances of the method for a growing number of parcels without any assumption on the anatomical relevance of the obtained parcels.

3.3 Quantitative validation

In order to avoid over-fitting, 28 brain surfaces belonging to $S_1 \backslash S_2$ are used as a training set. Since the cortical surfaces have not been registered, they all present different topologies and

node numbers. Table 1 summarizes the results in terms of reproducibility, sensitivity and specificity indices for all the 38 brains of the testing set, with different numbers of clusters.

As seen through the reproducibility index, even for a high number of parcels, performances remain good. Our Sensitivity and Specificity indices illustrate the stability of the quality of the parcellation, even for a high number of parcels. As expected, the performance decreases as the number of clusters increases but remains high even for a number of clusters equal to 40.

4. CONCLUSION AND DISCUSSION

In this work, we propose a novel fetal cortical surface parcellation and learning framework based on a mesh signature combining both *extrinsic* and *intrinsic* geometrical information. This mesh signature is first used in a joint-segmentation framework on all the cortical meshes to define a coherent parcellation on the surface of the brain. It is then used to learn and propagate this parcellation. The method is fully automatic, computationally low consuming, and allows for a multi-resolution parcellation of the fetal brain as the number of clusters to be used is chosen by the user. As a solution to the inherent lack of consistent anatomical brain features present across gestation, we propose a geometrically-based alternative to anatomical atlas-based methods. Both qualitative and quantitative validations demonstrate the robust performance of the proposed method. However, being based solely on a joint-segmentation of the whole training set at once, the parcellation, while spatially coherent, tends not to take into account the local variabilities with respect to anatomy. Moreover, in the proposed method each cerebral hemisphere is processed separately and thus there is no correspondence between both parcellations. We plan to address both of these limitations in our future work.

Acknowledgments

This work has been funded by the NIH-RO1HL116585 grant.

REFERENCES

1. Fischl B, Van der Kouwe A, Destrieux C, Halgren E, Ségonne F, Salat D, Busa E, Seidman L, Goldstein J, Kennedy D, Caviness V, Makris N, Rosen B, Dale A. Automatically parcellating the human cerebral cortex. Cerebral Cortex. 2004; 14:11–22. [PubMed: 14654453]
2. MacDonald D, Kabani N, Avis D, Evans AC. Automated 3-d extraction of inner and outer surfaces of cerebral cortex from MRI. Neuroimage. 2000; 12:340–356. [PubMed: 10944416]
3. Clouchoux C, Kudelski D, Gholipour A, Warfield SK, Viseur S, Bouyssi-Kobar M, Mari J-L, Evans AC, du Plessis AJ, Limperopoulos C. Quantitative in vivo MRI measurement of cortical development in the fetus. Brain structure & function. 2012; 217(1):127–139. [PubMed: 21562906]
4. Auzias, G.; De Guio, F.; Pepe, A.; Rousseau, F.; Mangin, J-F.; Girard, N.; Lefèvre, J.; Coulon, O. Model-driven parameterization of fetal cortical surfaces; IEEE international symposium on Biomedical imaging; 2015.
5. Habas PA, Scott JA, Roosta A, Rajagopalan V, Kim K, Rousseau F, Barkovich AJ, Glenn OA, Studholme C. Early folding patterns and asymmetries of the normal human brain detected from in utero MRI. Cerebral cortex. 2012; 22(1):13–25. [PubMed: 21571694]
6. Pepe, A.; Auzias, G.; De Guio, F.; Rousseau, F.; Germanaud, D.; Mangin, J.; Girard, N.; Coulon, O.; Lefevre, J. Spectral clustering based parcellation of fetal brain mri; IEEE international symposium on Biomedical imaging; 2015.

7. Lombaert H, Grady L, Polimeni JR, Cheriet F. Focusr: Feature oriented correspondence using spectral regularization-a method for precise surface matching. IEEE Transactions on Pattern Analysis and Machine Intelligence. 2013; 35(9):2143–2160. [PubMed: 23868776]
8. Mateus, D.; Horaud, R.; Knossow, D.; Cuzzolin, F.; Boyer, E. Articulated shape matching using Laplacian eigenfunctions and unsupervised point registration; IEEE Conference on Computer Vision and Pattern Recognition; 2008. p. 1-8.
9. Litman R, Bronstein AM. Learning spectral descriptors for deformable shape correspondence. IEEE Transactions on Pattern Analysis and Machine Intelligence. 2014; 36(1):171–180. [PubMed: 24231874]
10. Sun J, Ovsjanikov M, Guibas LJ. A concise and provably informative multi-scale signature based on heat diffusion. Computer Graphics Forum. 2009; 28(5):1383–1392.
11. Aubry, M.; Schlickewei, U.; Cremers, D. The wave kernel signature: A quantum mechanical approach to shape analysis; IEEE International Conference on Computer Vision Workshops (ICCV Workshops; 2011. p. 1626-1633.
12. Breiman L. Random forests. Machine Learning. 2001; 45(1):5–32.
13. Zabih, R.; Kolmogorov, V. Spatially coherent clustering using graph cuts; IEEE International Conference on Computer Vision and Pattern Recognition; 2004. p. 437-444.
14. Arthur, D.; Vassilvitskii, S. K-means++: the advantages of careful seeding; ACM-SIAM Symposium on Discrete Algorithms; 2007.
15. Lombaert, H.; Criminisi, A.; Ayache, N. Medical Image Computing and Computer Assisted Intervention (MICCAI)]. Springer; 2015. Spectral forests: Learning of surface data, application to cortical parcellation.
16. Meng, Y.; Li, G.; Gao, Y.; Shen, D. Automatic parcellation of cortical surfaces using random forests; IEEE International Symposium on Biomedical Imaging; 2015. p. 810-813.
17. Shapira L, Shamir A, Cohen-Or D. Consistent mesh partitioning and skeletonisation using the shape diameter function. The Visual Computer. 2008; 24(4):249–259.
18. Clouchoux C, du Plessis A, Bouyssi-Kobar M, Tworetzky W, McElhinney D, Brown D, Gholipour A, Kudelski D, Warfield S, McCarter R, Robertson R, Evans A, Newburger J, Limperopoulos C. Delayed cortical development in fetuses with complex congenital heart disease. Cerebral Cortex. 2013; 23(12):2932–2943. [PubMed: 22977063]
19. Shattuck D, Leahy R. Automated graph-based analysis and correction of cortical volume topology. IEEE Transactions on Medical Imaging. 2001; 20(11):1167–1177. [PubMed: 11700742]

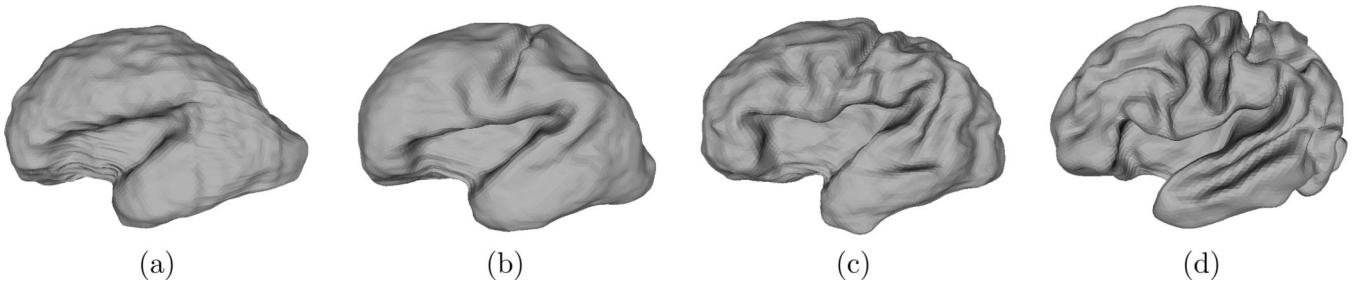

Figure 1.
Left hemisphere suface of a (a) 26 week gestational age (GA) fetus (b) 28 week GA fetus (c) 30 week GA fetus and (d) 34 week GA fetus.

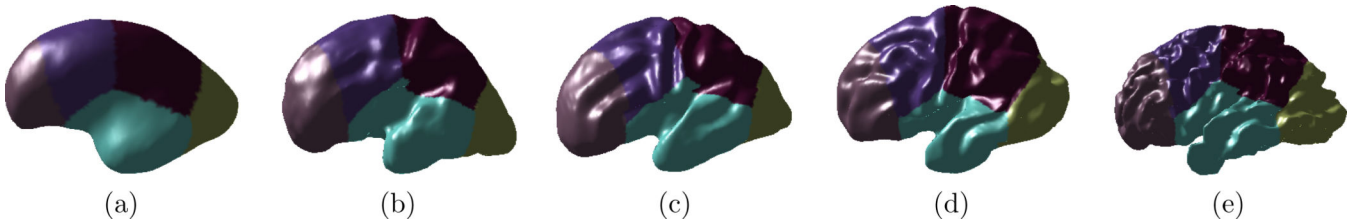

Figure 2.
Left hemisphere parcellation into 5 classes from a (a) 20 week gestational age (GA) fetus (b) 27 week GA fetus (c) 30 week GA fetus (d) 32 week GA fetus and (e) 37 week GA fetus.

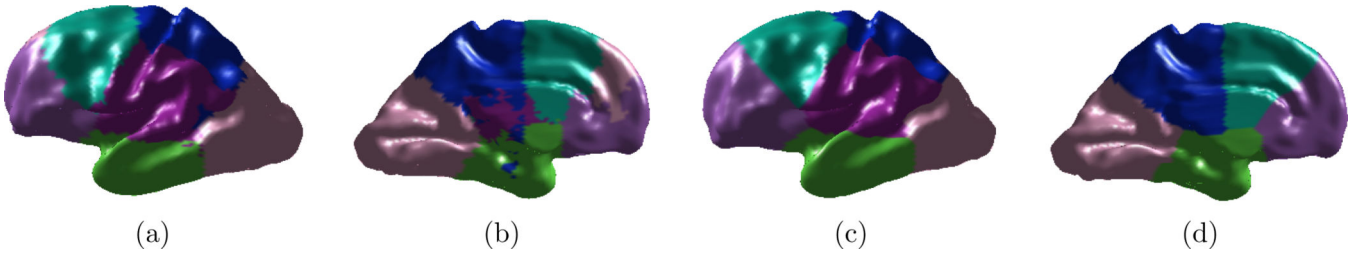

Figure 3.
Left cerebral hemisphere parcellation into 6 classes in a (a-b) 29 week GA fetus after RF, and (c-d) after graph-cuts.

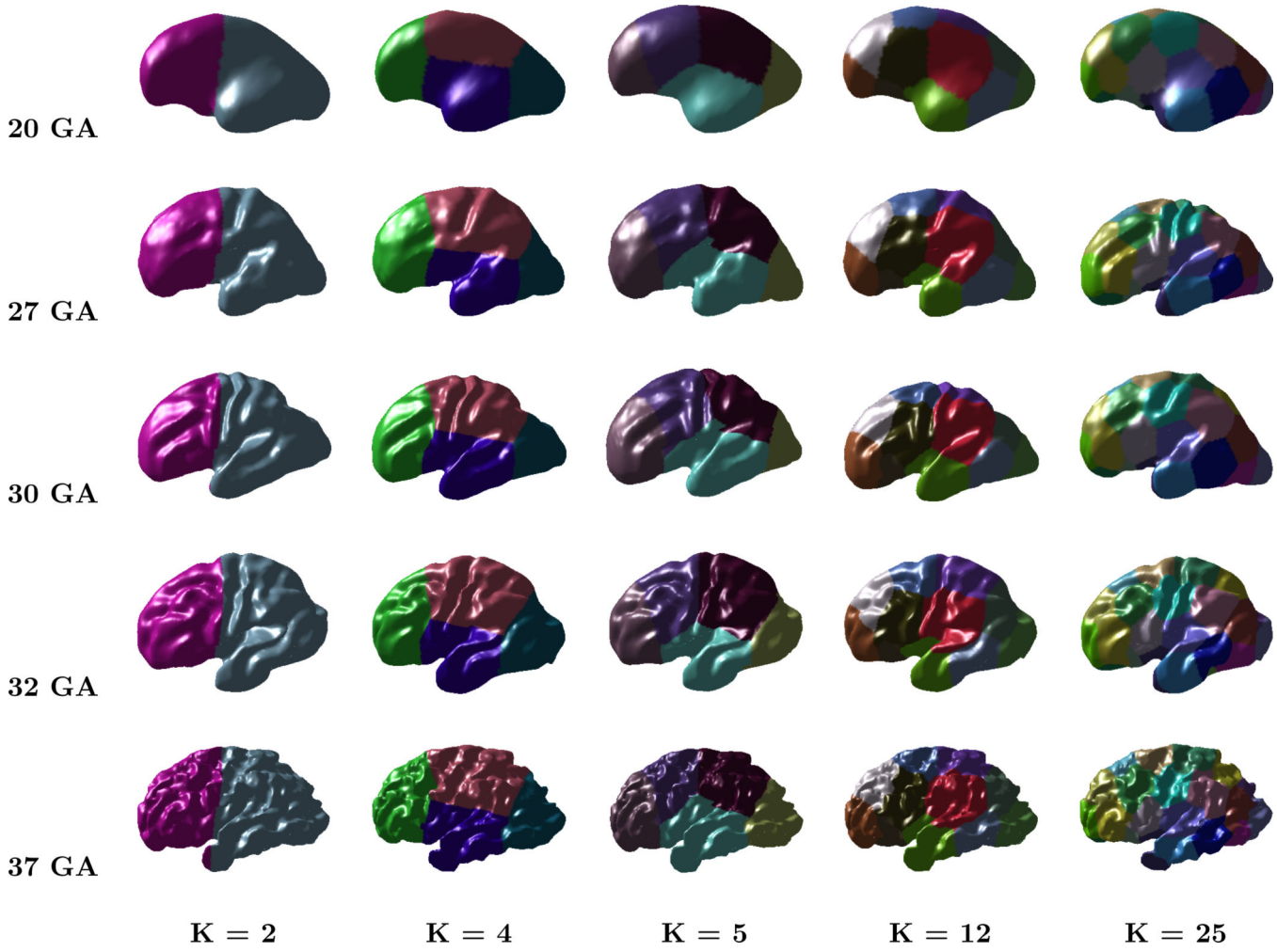

Figure 4.
Left hemisphere parcellation for fetuses at different gestational ages and for different number of clusters *K*.

Table 1

Quantitative Results

K	2	4	6	12	25	40
D_R index	0.98	0.94	0.93	0.87	0.84	0.78
Sensitivity index	0.98	0.98	0.98	0.99	0.99	0.99
Specificity index	0.98	0.94	0.92	0.87	0.82	0.77